

Phase transition temperatures determined by different experimental methods: Si(111)4×1-In surface with defects

Takahide Shibusaki,¹ Naoka Nagamura,¹ Toru Hirahara,^{1,*} Hiroyuki Okino,^{1,†} Shiro Yamazaki,^{1,‡} Woosang Lee,² Hyungjoon Shim,² Rei Hobara,¹ Iwao Matsuda,^{1,§} Geunseop Lee,^{2,||} and Shuji Hasegawa¹

¹*Department of Physics, University of Tokyo, 7-3-1 Hongo, Bunkyo-ku, Tokyo 113-0033, Japan*

²*Department of Physics, Inha University, Incheon 402-751, Korea*

(Received 2 October 2009; revised manuscript received 2 December 2009; published 11 January 2010)

The role of defects in the metal-insulator transition of a quasi-one-dimensional metallic surface Si(111)4×1-In, is investigated by temperature-dependent reflection high-energy electron diffraction (RHEED) spot analysis and microfour-point-probe (MFPP) surface conductivity measurements. In the RHEED spot intensity analysis, we found that adsorption of hydrogen or indium decreases the structural transition temperature into the 8×2 phase whereas it increases in the case of oxygen adsorption. In the MFPP, however, the metal-insulator transition temperature increased compared to that of the pristine surface universally irrespective of the additional atoms adsorbed as defects. The discrepancy between the two methods is discussed in terms of how the defects influence the metallic percolation path and formation of long-range order across the one-dimensional chains. Our results indicate that proper care should be taken concerning what each experimental method monitors when discussing phase transition phenomenon with various techniques.

DOI: [10.1103/PhysRevB.81.035314](https://doi.org/10.1103/PhysRevB.81.035314)

PACS number(s): 68.35.-p, 73.20.-r, 73.25.+i

I. INTRODUCTION

Historically, phase transitions have attracted much interest along with the development of thermodynamics or statistical physics. Melting and freezing of matter are among the most common yet fascinating physical phenomena and the history of the study stretches back more than one hundred years.¹ Nowadays we know that spontaneous breaking of symmetry is a concept employed not only in condensed matter physics but also in particle and astrophysics. In solid state physics, we learn that intriguing quantum physical phenomena such as superconductivity, superfluidity, or ferromagnetism arise as a consequence of the collective change in the electrons constituting the whole system.

Recently, there has been growing interest in phase transition phenomena of metal adsorbed semiconductor surfaces. These systems are excellent platforms to explore low-dimensional physics at the atomic scale. They have the advantage that the phase transition can be observed in real space with a scanning tunneling microscope (STM).² For example, from extensive electronic and transport studies, it has been reported that quasi-one-dimensional systems with arrays of Au atomic chains formed on a vicinal silicon wafer undergo a Peierls transition³ at low temperatures and become insulating.⁴⁻⁶ The Sn/Si(111) or Ge(111) systems have been reported to show a Mott transition at low temperatures which is still under debate.⁷⁻¹¹

In this study, we have employed the well-known Si(111)4×1-In surface as a platform to study the role of atomic scale defects in the phase transition phenomenon. This surface is metallic at room temperature but shows structural and electronic phase transitions by turning into an insulating 8×2 phase, both occurring simultaneously at the same temperature around ~120 K.¹²⁻¹⁴ Extensive work has been performed to identify the nature of this phase transition and basically two major explanations have been made. One is a Peierls-instability driven charge-density wave (CDW)

formation in which a metallic and structurally static 4×1 phase turns into an insulating 8×2 phase (order-order transition).^{14,15} The other is an order-disorder transition where the apparent 4×1 phase at room-temperature results from the dynamic fluctuation of the insulating 8×2 (or the 4×2) phase. In this order-disorder transition scenario, the metallicity of the 4×1 phase at room temperature is induced by the shear motion of the In zigzag rows of the insulating 8×2 (or the 4×2) phase at low temperature.^{16,17}

In the past there have been some works published that have investigated the role of defects in this phase transition.¹⁸⁻²² Sodium (Na) adsorption was found to induce the insulating 4×2 phase even at room temperature.²³ STM and reflection high-energy electron diffraction (RHEED) studies showed that tiny amounts of Ag or In on the low temperature 8×2 phase reverted the surface back to 4×1, meaning that the transition temperature has decreased.¹⁹ In a series of low-energy electron diffraction (LEED) studies, it was found that Na, H, and In adatoms lowered the phase transition temperature while only O was shown to increase it.²⁴⁻²⁶ On the other hand, the metal-insulator (MI) transition temperature found in surface-sensitive conductivity measurements increased for the additional In-adsorbed surface compared to the pristine 4×1.¹³

With all these confusions in the results from different measurements, there is no consensus up to now as to how the defects influence the phase transition on this system. Therefore we have carried out a comparative study on the role of defects (H, O, and In adatoms) both using temperature-dependent RHEED spot intensity analysis and micro-four-point probe (MFPP) conductivity measurements to obtain a comprehensive understanding. Temperature-dependent RHEED spot profile analysis showed that the structural transition to the 8×2 phase occurs at a lower temperature for the H and In adsorptions, whereas the transition temperature increases with O exposure. This is in good agreement with previous LEED studies.²⁴⁻²⁶ However, the metal-insulator

transition temperature determined by MFPP conductivity measurements was found to increase compared with the pristine Si(111)4×1-In surface irrespective of the defect elements studied. This shows that the metallic percolation path can disappear without the long-range order of the low-temperature phase. Our results suggest the importance to identify carefully what each experimental technique monitors in phase transition studies.

II. EXPERIMENTAL

An *n* type (resistivity of 1–10 Ω cm at 300 K) Si(111) wafer with a miscut of 1.8° along the $[\bar{1}\bar{1}2]$ direction was used as the substrate. The Si(111)-7×7 clean surface was prepared by direct current heating up to 1500 K for a few seconds. The Si(111)4×1-In surface was formed by one ML (7.83×10^{14} atoms/cm²) indium deposition onto the 7×7 surface at 450 °C. The sample temperature below room temperature was monitored by a thermal couple (TC) attached close to the sample holder and the difference between the actual sample temperature and the TC is within ±5 °C.

The RHEED patterns ($[11\bar{2}]$ incident) were recorded continuously by a charge-coupled device camera to monitor the structure change at the phase transition while cooling the sample in an ultrahigh vacuum (UHV) chamber. Oxygen gas was dosed at room temperature by backfilling the chambers. Hydrogen exposure was done also at room temperature by cracking the gas with a heated tungsten filament. One Langmuir (L) corresponds to 1×10^6 Torr s. The conductivity measurements were performed using a separate custom-made UHV chamber for *in situ* MFPP measurement.²⁷ The probe spacing was 20 μm and the resistance was measured while cooling down the sample from room temperature.

III. RESULTS

A. Phase-transition temperature determined by temperature-dependent RHEED spot intensity analysis

In order to gain insight into the influence of defects on the structural transition of Si(111)4×1-In surface, we begin with the results of the temperature-dependent RHEED spot intensity analysis. Figure 1(a) shows the RHEED pattern of the 8×2 phase obtained for the surface without defects at 50 K. In the analysis we have monitored the spot intensity of the (3/8 5/8) spot and have integrated the intensity of the region surrounded by the rectangle in Fig. 1(a). Figures 1(b)–1(d) show the temperature dependence of the RHEED spot intensity for the additional (b) In, (c) H, and (d) O adsorptions, respectively. The arrows indicate the point where the structural phase transition occurred (T_c^{RHEED}) and the horizontal lines show zero level. For indium [Fig. 1(b)] and hydrogen [Fig. 1(c)], we see that as more defects are introduced on the surface, the eighth-order spots appear at lower temperatures (for example, 80 K for the 0.5 L H exposed surface and 72 K for the 0.02 ML In-adsorbed surface) compared to 110 K at the pristine surface. In Fig. 1(d), however, we see that as the oxygen exposure increases, the temperature that the eighth-order spots appear rises accordingly, namely, 110 K for the

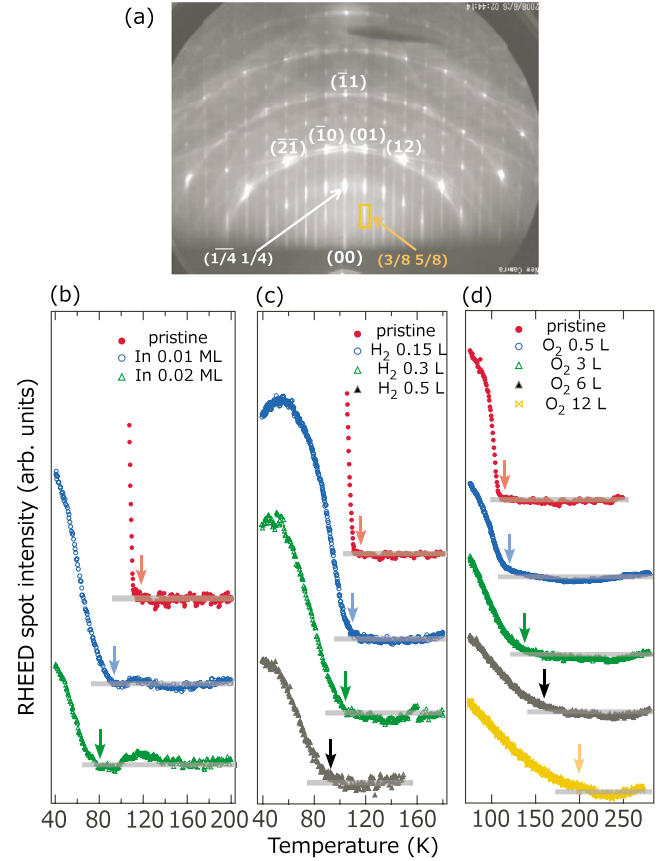


FIG. 1. (Color online) (a) The RHEED pattern of the Si(111)8×2-In phase. The beam is incident along the $[11\bar{2}]$ direction and the electron energy is 15 keV. (b), (c), and (d) The temperature dependence of the RHEED spot intensity for the eighth order spot (3/8 5/8) surrounded by the rectangle in (a). The arrows indicate the occurrence of the phase transition and the horizontal lines show zero level.

pristine surface and 200 K for the surface exposed to 12 L of oxygen, for example. These results are consistent with the recent LEED observations showing that adsorption of O increases the transition temperature while In, H, and Na decreases it.^{24–26}

B. Influence of defects on the surface-state conductivity at room temperature

To evaluate the influence of defects on the electrical properties of the surface, first we have investigated how the defects affect the surface-state electrical conductivity. Figure 2(a) shows the resistance change in the Si(111)4×1-In surface as a function of the gas exposure for hydrogen (open symbols) and oxygen (filled symbols) cases. One can see that the resistance increases with gas exposure, meaning that the surface conductivity of the Si(111)4×1-In surface decreases with gas adsorption. Independent analyses of the defects using STM images [representative images of the surfaces with H and O defects are shown in Figs. 2(b) and 2(c), respectively] showed that the defect density increases linearly with gas exposure for both H and O [indicated by the solid lines

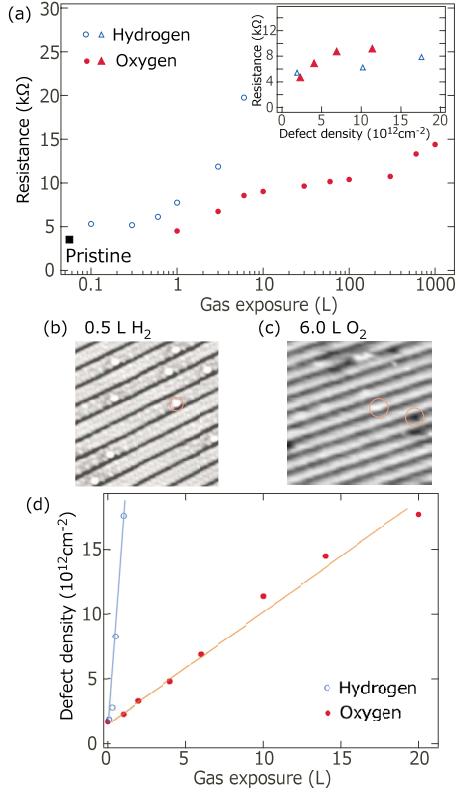


FIG. 2. (Color online) (a) Surface resistance change as a function of the gas exposure for the Si(111) 4×1 -In surface. The solid circles are the data for oxygen exposure and open circles are those for hydrogen exposure. The inset shows the surface resistance replotted as a function of the defect density for both cases. (b) and (c) STM images ($125 \times 125 \text{ \AA}^2$) after (b) 0.5 L of hydrogen exposure and (c) 6 L of oxygen exposure, respectively. The circles indicate the induced defects. (d) The defect density estimated from STM images as a function of gas exposure.

in Fig. 2(d)]. In the case of H adsorption defects that appear bright are seen, while for O both bright and dark ones are seen.²⁴ The number (density) of defects induced by H exposure appears to increase much faster than that with O exposure. This is probably because of the difference in the effectiveness of inducing each adsorption, i.e., atomic H is formed by cracking but oxygen is only backfilled and dissociates spontaneously. It may also be attributed to the difference in the local surface structure around defects.²⁰ Using the relation between the gas exposure and the defect density, the increase in the resistance with gas-induced defects can be redrawn [inset in Fig. 2(a) with x axis as the defect density]. In this plot, the resistance is roughly a simple function of defect density. This is in agreement with Ref. 18 in which the authors showed that the anisotropy of the surface-state conductivity decreased by oxygen adsorption due to the increased defect density at the surface. We can also see that hydrogen is as effective in decreasing the surface conductivity as oxygen. This is apparently in contradiction to the theoretical work of Wippermann *et al.*²² in which they showed that H has minimum effect on the surface-state conductance (4% reduction), whereas for O the combination of potential-well scattering and nanowire deformation reduces the

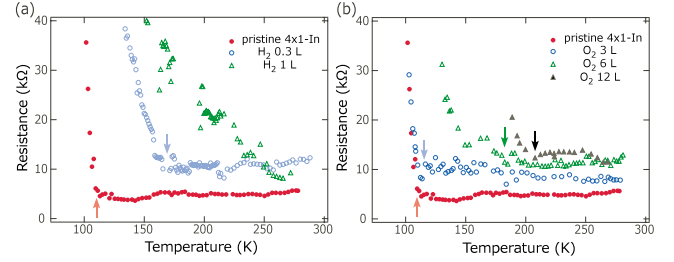


FIG. 3. (Color online) (a) The temperature dependence of the surface resistance for the pristine and H₂ exposed Si(111) 4×1 -In surfaces. (b) Those for the pristine and O₂ exposed Si(111) 4×1 -In surfaces. The arrows indicate the occurrence of the phase transition.

surface-state conductance significantly. The calculation in Ref. 22 considered high concentration of defects with one defect per a 4×1 unit cell, whereas cases of very low concentrations of the defects (“impurity” regime) have been studied in the experiment. Therefore we believe the calculation has no correspondence to the experiment and the two cannot be compared directly.

C. Phase-transition temperature determined by temperature-dependent conductivity measurements

Next we discuss the influence of defects on the metal-insulator (MI) transition temperature measured by the surface conductivity change. Figures 3(a) and 3(b) show the temperature dependence of the measured resistance as a function of temperature for the (a) hydrogen and (b) oxygen exposure cases, respectively. Different symbols show the data set for different gas exposures. Also shown is the data for the pristine Si(111) 4×1 -In surface. The arrows indicate the temperature that the MI transition occurred (T_c^{MFPP}). From Fig. 3(a) we can see that T_c^{MFPP} rises for the 0.3 L H₂ exposed surface (159 K) compared with the pristine surface (115 K). For the 1 L exposed surface, the MI transition is not evident as the resistance already rises from room temperature, so we can say that T_c^{MFPP} is higher than room temperature. In Fig. 3(b), we also find that T_c^{MFPP} rises with increasing oxygen exposure, namely 115, 120, 180, and 205 K for the pristine, 3, 6, and 12 L exposed surfaces, respectively. A similar study has been reported for additional In adsorption on the Si(111) 4×1 -In surface.¹³ The authors found that by 0.1 ML additional In deposition on the pristine 4×1 -In phase at room temperature, the conductivity is significantly decreased and T_c^{MFPP} rises to 160 K.²⁸ This is the same tendency we have observed for the above H and O cases in this study. So as a consequence, we can say that the surface-state conductivity is greatly decreased by defects and the MI transition temperature rises compared with the pristine surface.

We have also checked the RHEED pattern just after the MI transition (at a temperature slightly below T_c^{MFPP}). For the pristine surface, it showed the well-known 8×2 periodicity. However, for the O and H 0.3 L exposed surfaces, it only showed the 4×2 pattern without the $\times 8$ spots, meaning that the interchain correlation was not formed on these surfaces at this MI transition temperature. It was also reported

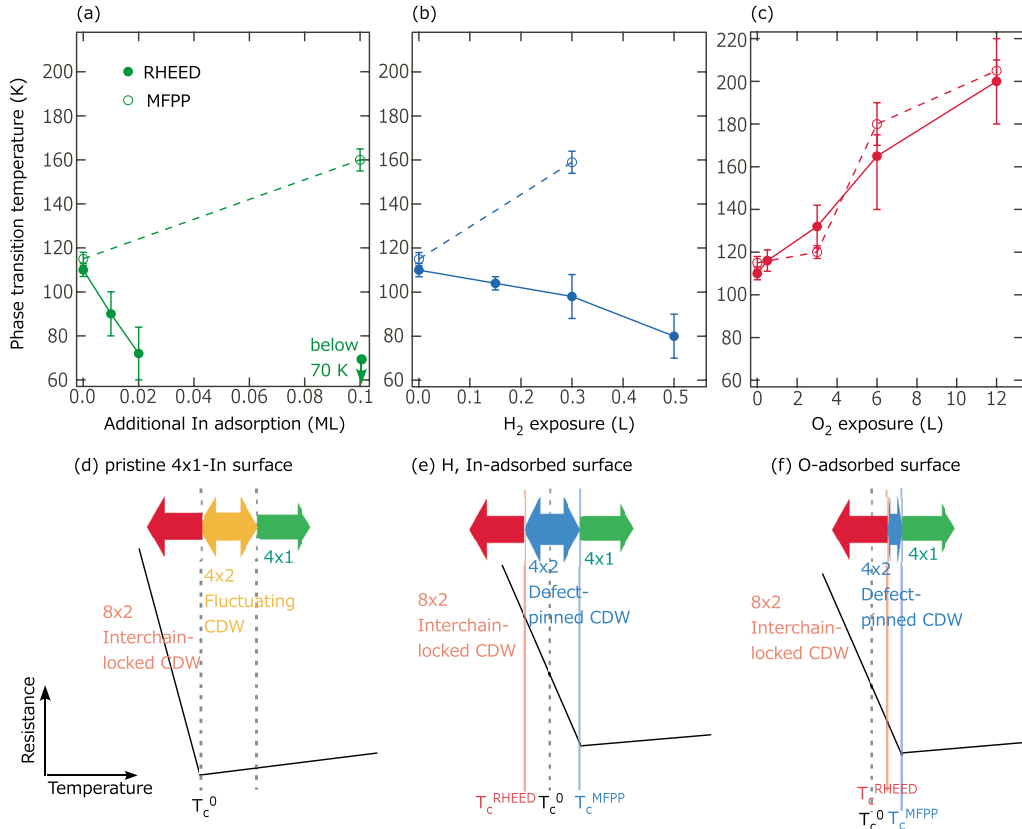


FIG. 4. (Color online) (a), (b), and (c) The phase transition temperatures deduced from RHEED intensity of Fig. 1 (filled circles with error bars) and MFPP conductivity measurements of Fig. 3 (open circles with error bars) for additional In adsorption (a), H₂ exposure (b), and O₂ exposure (c), respectively. The solid and dotted lines show the guide to the eye. (d), (e), and (f) The schematic drawings of the relationship between the “phase transition temperature” determined by RHEED measurements (T_c^{RHEED}), MFPP conductivity measurements (T_c^{MFPP}) and that for the pristine surface (T_c^0) for the pristine (d), H or In-adsorbed surfaces (e), and O-adsorbed surfaces (f). For the pristine surface, $T_c^0 = T_c^{RHEED} = T_c^{MFPP}$ (by notifying that the transition temperature is determined by the eighth-order spot intensity).

that for the additional In case, it only showed a 4×2 pattern after the phase transition.²⁹ This is quite interesting because the conductivity starts to show an insulating behavior even though the structural phase transition has not yet occurred for the defected surfaces. This suggests that *the MI transition observed in the conductivity measurements is not the actual structural transition to the 8×2 phase.*

IV. DISCUSSION: THE RELATION BETWEEN T_c^{RHEED} AND T_c^{MFPP}

Figure 4 summarizes the results we have obtained in the previous sections. It shows the relationship between the phase transition temperatures determined with RHEED spot intensity analysis (T_c^{RHEED} , open circles) and those obtained by conductivity measurements (T_c^{MFPP} , filled circles) for indium [Fig. 4(a)], hydrogen [Fig. 4(b)], and oxygen [Fig. 4(c)] adsorption, respectively. For oxygen, both T_c^{MFPP} and T_c^{RHEED} increase compared to the pristine surface, whereas for H and In, T_c^{MFPP} rises but T_c^{RHEED} falls. When we compare O and H, H has much more effect on the transition temperature compared to O if the dosage is the same which is due to the higher efficiency of H to induce defects at the surface. The RHEED results about the influence of defects

on the phase transition temperature are consistent with those of LEED.^{24,25} So now it is obvious that we have to distinguish the “transition” determined by the two methods, diffraction, and electrical measurements.

Previously, a scenario based on the picture of the CDW phase transition has been provided to explain the change in the structural phase transition temperature.²⁴ Based on the same picture, we now attempt to provide an explanation compromising the difference in the phase transition temperature seen by RHEED and MFPP measurements in the following. First, let us consider the case of a pristine Si(111)4 \times 1-In. When the surface is cooled, one-dimensional (1D) CDWs with a doubled ($\times 2$) periodicity along the chain start to form. Formation of these 1D CDWs has been experimentally observed not only in real space^{30,31} but also in momentum space¹³ as a 4×2 RHEED pattern developed around 160 K. However, the conductivity was not much affected at this temperature. It is because these 1D CDWs are fluctuating, i.e., not fixed in space and time,^{30,31} and thus metallic conducting paths are still available for electron transport. Such fluctuation has indeed been observed in STM observations.³⁰ Upon further cooling down, these fluctuations become suppressed to form rather stationary two-dimensional (2D) islands of insulating 8×2 phase. When 2D islands of the 8×2 phase has grown sufficiently to cut the passage of the

metallic 4×1 phase (the percolation of the 4×1 phase is no longer available), the surface-state resistance increases steeply. Therefore, T_c^{MFPP} and T_c^{RHEED} are nearly the same¹³ and we will call this T_c^0 here. This situation is schematically illustrated in Fig. 4(d).

Now let us consider the case with additional H or In defects added on the surface [Fig. 4(e)]. As reported in Refs. 20 and 21, the surface remains metallic even around these defects. When the sample is cooled down, a 4×2 RHEED pattern will arise due to the formation of 1D CDWs within a single chain which is similar to the clean surface. However, these CDWs cannot fluctuate as they are pinned by the defects on the surface. As the temperature is lowered further, more defect-pinned CDWs are formed and they also become connected in the direction perpendicular to the chain without having the $\times 8$ periodicity due to the pinning effect by the defects. When these 2D insulating islands without 8×2 order across the chains become dominant on the surface and a metallic percolation no longer exists, the resistance will start to increase rapidly. This happens at a temperature higher than T_{c0} because of the suppression of the fluctuation ($T_c^{MFPP} > T_c^0$). A similar situation may occur in the order-disorder transition scenario by the pinning of the dynamical fluctuation by defects. It should be emphasized that our results indicate that at this temperature, the formation of rather well-ordered 2D islands of the 8×2 structure does not yet occur. This is probably because the pinning effect by randomly distributed defects (causing disorder in the $\times 8$ periodicity across the chains) is much stronger than the interchain coupling on the pristine surface which favors the $\times 8$ periodicity. In order for the interchain coupling effect to overcome the defect pinning effect, we believe that the temperature must be lowered than T_c^0 considering the entropic contribution in the free energy. This scenario presumably explains why T_c^{RHEED} is lower than T_c^0 in the case of H and In defects.

The conductivity data can also be explained in an alternative way in terms of hopping conduction on defect-rich one-dimensional systems.³² Around defects, a 1D Friedel oscillation occurs which creates additional scattering potentials for the conducting electrons. This is the main reason for the decrease in the conductivity when we present defects. However a metallic path can be still seen at temperatures near RT, because there are some regions where the pristine 4×1 -In surface is present and the electrons can hop to the neighboring chains. By cooling, the decay constant (coherent length) of the Friedel oscillation extends. When the Friedel oscillation sufficiently covers the surface so that a metallic path is no longer available (even when the electrons hop to the adjacent chains, the pristine 4×1 -In surface is not present), the resistance starts rising.³³ Because the Friedel oscillation also shows a $\times 2$ periodicity along the chains (4×2), we cannot actually make a clear distinction between a metal-insulator transition due to a “defect-pinned CDW” (“defect-pinned ordered insulating ground state”) and a “localization effect induced by the Friedel oscillation” in terms of conductivity measurements.

The above arguments can suitably explain the $T_c^{MFPP} > T_c^0$ for all the defects we studied here (H, In, and O) and $T_c^0 > T_c^{RHEED}$ found in the cases of H and In, except for O [Fig. 4(f)]. Speculative scenarios have been proposed to ac-

count for the exceptional increase in the transition temperature of the O-defected surface in the LEED measurements.²⁴ According to those scenarios, the defects induced by O may in some way rearrange themselves to make regular distribution with $\times 8$ periodicity, or alternatively plays as an acceptor (providing holes) to make the transition into the 8×2 phase preferable. These scenarios are also applicable for the RHEED measurements in the present study. To test these speculative scenarios, extensive detailed experiments concerning the distribution of defects in real space, or the defect-induced changes of the Fermi surface as well as the gap size are needed. Further elaborate studies are called for resolving this intricate mechanism of the change in the phase transition temperature.

The difference of “transition temperature” determined by different experimental methods was also discussed for the Si(553)-Au surface,⁶ which has much more inherent defects than the present Si(111) 4×1 -In surface and is also said to undergo a Peierls instability.⁴ ARPES reported that the transition temperature was ~ 250 K, while STS reported that it occurs below 110 K,³⁴ and MFPP measurements showed a metal-insulator transition at ~ 160 K. Of course there is a possibility that the defect density is not the same in different measurements, but an alternative explanation given by the authors in Ref. 6 was that ARPES probes the onset of the development of the insulating region, while STS observes the complete disappearance of the metallic region (the STS spectra shown in Ref. 34 were spatially averaged) while the MFPP conductivity measurements detect the loss of the metallic percolation path. The present study and Ref. 6 clearly show that it is necessary to consider thoroughly what each experimental method is monitoring in temperature-dependent phase transition studies.

V. CONCLUSION

In summary, we have investigated how defects influence the phase transition of the Si(111) 4×1 -In surface by adsorbing hydrogen, oxygen, or additional indium. Compared with the case of the pristine surface, the *structural* phase transition temperature decreased with H or In adsorbates, but increased with O-induced defects. These apparently conflicting results indicate diverse roles of different defects in the phase transition. In contrast, the defects commonly increased the *metal-insulator* transition temperatures. It was attributed to the universal role of the defects, which suppress the fluctuations of the insulating phase (4×2) by pinning and enhance the connectivity of the 2D condensations. The metallic percolation may disappear, resulting in the universal increase in the metal-insulator transition temperature even without building the long-range order across the chains of the low-temperature structure. The results in this study that the structural and electrical phase transitions do not occur simultaneously emphasize the importance of careful consideration of what is monitored when a specific experimental method is used in investigating the phase transition phenomenon.

ACKNOWLEDGMENTS

This work has been supported by Grants-In-Aid, Japan-Korea Joint Research Project, and A3 Foresight Program from Japanese Society for the Promotion of Science. G.L.

was supported by grants from the Korea-Japan Joint Research Program (F01-2005-000-10279-0) and Quantum Metamaterials Research Center (R11-2008-053-02001-0) through the Korea Science and Engineering Foundation funded by the Korean Government (MEST).

*hirahara@surface.phys.s.u-tokyo.ac.jp

[†]Present address: Hitachi Ltd., Kokubunji, Japan.

[‡]Present address: Institute of Applied Physics and Microstructure Research Center, University of Hamburg, Jungiusstrasse 11, 20355 Hamburg, Germany.

[§]Present address: Institute for Solid State Physics, University of Tokyo, Chiba 277-8581, Japan.

^{||}glee@inha.ac.kr

¹J. G. Dash, *Rev. Mod. Phys.* **71**, 1737 (1999).

²J. M. Carpinelli, H. H. Weitering, E. W. Plummer, and R. Stumpf, *Nature (London)* **381**, 398 (1996).

³George Grüner, *Density Waves in Solids* (Addison-Wesley, Reading, MA, 1994).

⁴J. R. Ahn, P. G. Kang, K. D. Ryang, and H. W. Yeom, *Phys. Rev. Lett.* **95**, 196402 (2005).

⁵J. R. Ahn, H. W. Yeom, H. S. Yoon, and I.-W. Lyo, *Phys. Rev. Lett.* **91**, 196403 (2003).

⁶H. Okino, I. Matsuda, S. Yamazaki, R. Hobara, and S. Hasegawa, *Phys. Rev. B* **76**, 035424 (2007).

⁷G. Profeta and E. Tosatti, *Phys. Rev. Lett.* **98**, 086401 (2007).

⁸S. Modesti, L. Petaccia, G. Ceballos, I. Vobornik, G. Panaccione, G. Rossi, L. Ottaviano, R. Larciprete, S. Lizzit, and A. Goldoni, *Phys. Rev. Lett.* **98**, 126401 (2007).

⁹R. Cortés, A. Tejada, J. Lobo, C. Didiot, B. Kierren, D. Malterre, E. G. Michel, and A. Mascaraque, *Phys. Rev. Lett.* **96**, 126103 (2006).

¹⁰H. Morikawa, S. Jeong, and H. W. Yeom, *Phys. Rev. B* **78**, 245307 (2008).

¹¹S. Colonna, F. Ronci, A. Cricenti, and G. Le Lay, *Phys. Rev. Lett.* **101**, 186102 (2008).

¹²T. Uchihashi and U. Rampsberger, *Appl. Phys. Lett.* **80**, 4169 (2002).

¹³T. Tanikawa, I. Matsuda, T. Kanagawa, and S. Hasegawa, *Phys. Rev. Lett.* **93**, 016801 (2004).

¹⁴H. W. Yeom, S. Takeda, E. Rotenberg, I. Matsuda, K. Horikoshi, J. Schaefer, C. M. Lee, S. D. Kevan, T. Ohta, T. Nagao, and S. Hasegawa, *Phys. Rev. Lett.* **82**, 4898 (1999).

¹⁵J. R. Ahn, J. H. Byun, H. Koh, E. Rotenberg, S. D. Kevan, and H. W. Yeom, *Phys. Rev. Lett.* **93**, 106401 (2004).

¹⁶C. González, F. Flores, and J. Ortega, *Phys. Rev. Lett.* **96**, 136101 (2006).

¹⁷C. González, J. Guo, J. Ortega, F. Flores, and H. H. Weitering,

Phys. Rev. Lett. **102**, 115501 (2009).

¹⁸H. Okino, I. Matsuda, R. Hobara, S. Hasegawa, Y. Kim, and G. Lee, *Phys. Rev. B* **76**, 195418 (2007).

¹⁹S. V. Ryjkov, T. Nagao, V. G. Lifshits, and S. Hasegawa, *Surf. Sci.* **488**, 15 (2001).

²⁰G. Lee, S. Y. Yu, H. Kim, and J. Y. Koo, *Phys. Rev. B* **70**, 121304(R) (2004).

²¹G. Lee, S. Yu, D. Lee, H. Kim, and J. Koo, *Jpn. J. Appl. Phys.* **45**, 2087 (2006).

²²S. Wippermann, N. Koch, and W. G. Schmidt, *Phys. Rev. Lett.* **100**, 106802 (2008).

²³S. S. Lee, J. R. Ahn, N. D. Kim, J. H. Min, C. G. Hwang, J. W. Chung, H. W. Yeom, S. V. Ryjkov, and S. Hasegawa, *Phys. Rev. Lett.* **88**, 196401 (2002).

²⁴G. Lee, S. Y. Yu, H. Shim, W. Lee, and J. Y. Koo, *Phys. Rev. B* **80**, 075411 (2009).

²⁵H. Shim, S. Yu, W. Lee, J. Koo, and G. Lee, *Appl. Phys. Lett.* **94**, 231901 (2009).

²⁶H. Shim, W. Lee, and G. Lee (unpublished).

²⁷T. Tanikawa, I. Matsuda, R. Hobara, and S. Hasegawa, *e-J. Surf. Sci. Nanotechnol.* **1**, 50 (2003).

²⁸It should be noted that in Ref. 19, the conductivity has been found to increase by In adsorption. However, the additional In deposition was performed at 100K on the 8×2 surface and the 8×2 insulating phases reverted back into the 4×1 metallic phase, resulting in the increased conductivity. On the contrary, we deposited extra In at room temperature on the 4×1 metallic phase and found that the conductivity decreases. Therefore these two measurements are completely different experiments are not contradictory to each other.

²⁹T. Tanikawa, Doctoral thesis, University of Tokyo (2003).

³⁰G. Lee, J. Guo, and E. W. Plummer, *Phys. Rev. Lett.* **95**, 116103 (2005).

³¹S. J. Park, H. W. Yeom, J. R. Ahn, and I.-W. Lyo, *Phys. Rev. Lett.* **95**, 126102 (2005).

³²M. M. Fogler, S. Teber, and B. I. Shklovskii, *Phys. Rev. B* **69**, 035413 (2004).

³³I. Matsuda, C. Liu, T. Hirahara, M. Ueno, T. Tanikawa, T. Kanagawa, R. Hobara, S. Yamazaki, S. Hasegawa, and K. Kobayashi, *Phys. Rev. Lett.* **99**, 146805 (2007).

³⁴P. C. Snijders, S. Rogge, and H. H. Weitering, *Phys. Rev. Lett.* **96**, 076801 (2006).